Development 128, 2397-2406 (2001)
Printed in Great Britain © The Company of Biologists Limited 2001
DEV3398

Haploinsufficiency of the forkhead gene *Foxf1*, a target for sonic hedgehog signaling, causes lung and foregut malformations

Margit Mahlapuu[1], Sven Enerbäck[2] and Peter Carlsson[1]

[1]Department of Molecular Biology, Göteborg University, The Lundberg Laboratory, Box 462, SE-405 30 Göteborg, Sweden
[2]Department of Medical Biochemistry, Göteborg University, SE-405 30 Göteborg, Sweden
*Author for correspondence (e-mail: peter.carlsson@molbio.gu.se)

Accepted 10 April 2001

SUMMARY

The murine *Foxf1* gene, encoding a forkhead – or winged helix – transcription factor, is expressed in splanchnic mesenchyme during organogenesis. The concentration of expression to subepithelial mesenchyme suggested that *Foxf1* is activated by paracrine signals from endodermal epithelia. Homozygous *Foxf1*-null mice die before embryonic day 10, owing to defects in extra-embryonic mesoderm, and do not provide any information about the role of *Foxf1* in morphogenesis of endodermally derived organs. We show that, on CD1 genetic background, *Foxf1* heterozygote perinatal mortality is around 90%. The haploinsufficiency causes a variable phenotype that includes lung immaturity and hypoplasia, fusion of right lung lobes, narrowing of esophagus and trachea, esophageal atresia and tracheo-esophageal fistula. Similar malformations are observed in mutants that are defective in the sonic hedgehog (Shh) signaling pathway, and we show that exogenous Shh activates transcription of *Foxf1* in developing lung. *Foxf1* mRNA is absent in the lungs, foregut and sclerotomes of *Shh*$^{-/-}$ embryos, but persists in tissues where indian hedgehog (*Ihh*) is expressed. In lung organ cultures, activation of *Foxf1* by Shh is counteracted by bone morphogenetic protein 4 (BMP4). Fibroblast growth factor (FGF) 10 and FGF7 both decrease *Foxf1* expression and we speculate that this is mediated by transcriptional activation of epithelial *Bmp4* (in the case of FGF10) and by inhibition of *Shh* expression for FGF7.

Key words: Lung, Mouse, Foregut, *Foxf1*, forkhead

INTRODUCTION

Morphogenesis of the mammalian lungs and foregut is controlled by interactions between the endodermal epithelium and the surrounding mesenchyme. Grafting experiments have demonstrated the distinct inductive capacities of proximal and distal mesenchyme, derived from the trachea and the tips of the growing lungs, respectively (Wessells, 1970). In the last decade, several key components in the paracrine crosstalk between mesenchyme and epithelium have been identified.

Hedgehog proteins are secreted signaling molecules that are involved in many morphogenetic processes. In *Drosophila*, Hedgehog signaling is received by the cell surface receptor Patched and transduced by Smoothened, which modulates the transcription factor Cubitus interruptus (Ci) through control of its proteolytic processing (reviewed by Aza-Blanc and Kornberg, 1999). The essentials of this pathway appear to be conserved in mammals, which have three different hedgehog proteins, indian (Ihh), desert (Dhh) and sonic hedgehog (Shh); two Patched homologs, patched 1 (Ptch) and patched 2 (Ptch2); and three homologs of Ci, Gli1, Gli2 and Gli3 (reviewed by McMahon, 2000). *Shh* is the most widely expressed of the mammalian hedgehogs and is the only one expressed in lung and foregut (Bitgood and McMahon, 1995). *Shh* mRNA is found throughout the early respiratory epithelium, but high level expression is confined to the distal epithelium, near the tips of the growing buds (Bellusci et al., 1996; Urase et al., 1996). Gene targeting in mice, as well as transgenic overexpression, have demonstrated the importance of Shh for normal development and branching morphogenesis of the lungs (Bellusci et al., 1997a; Litingtung et al., 1998; Pepicelli et al., 1998). Inactivation of *Shh* or components in its signal transduction pathway, such as *Gli2* and *Gli3*, gives rise to various degrees of lung and foregut malformations, with fusion of lung lobes, hypoplasia and esophageal atresia or stenosis, but the mechanism behind these morphogenetic defects is unknown (Litingtung et al., 1998; Motoyama et al., 1998; Park et al., 2000; Pepicelli et al., 1998). Mesenchymal genes, whose expression depends on hedgehog signaling have been identified. Several of these encode proteins that themselves are part of the hedgehog signaling pathway (such as Ptch, Gli1 and Gli3). Other target genes encode paracrine factors that are known to take part in morphogenesis and can either be activated, such as *Wnt2*, or repressed, like *Fgf10*, by Shh (Bellusci et al., 1997b; Lebeche et al., 1999; Litingtung et al., 1998; Pepicelli et al., 1998). However, in many cases it remains to be shown if the effect is direct or mediated by other secreted proteins.

The forkhead genes *Foxf1* (also known as *FREAC1* or *HFH8*) and *Foxf2* (also known as *FREAC2* or *LUN*) encode

two transcription factors that are closely related with regard to primary structure, DNA binding specificity and expression pattern, but with distinct activating properties (Clevidence et al., 1994; Hellqvist et al., 1998; Hellqvist et al., 1996; Mahlapuu et al., 1998; Pierrou et al., 1994). Both genes are expressed during organogenesis in mesenchymal tissue derived from splanchnic mesoderm and sclerotomes (Aitola et al., 2000; Mahlapuu et al., 2001; Mahlapuu et al., 1998; Peterson et al., 1997). In developing lung and in several other endodermally derived organs, *Foxf1* and *Foxf2* mRNA is concentrated in subepithelial mesenchyme, which has prompted the speculation that their expression is induced by epithelial paracrine signaling (Aitola et al., 2000; Mahlapuu et al., 1998). We recently reported inactivation of *Foxf1* by gene targeting (Mahlapuu et al., 2001). However, homozygous *Foxf1*-null mice degenerate at the early somite stage and die before organogenesis begins; hence, they do not provide any information on the role of *Foxf1* in foregut or lung development. We show that *Foxf1* is activated by Shh signaling and that, on a specific genetic background, *Foxf1* haploinsufficiency gives rise to lung and foregut malformations similar to those observed in *Shh* and *Gli* mutants.

MATERIALS AND METHODS

Mouse mutants

A targeting construct containing a total of 12 kb of the *Foxf1* locus was made from 129/Sv genomic λ clones, in which the forkhead box of *Foxf1* (from *Sst*I to *Not*I) was replaced by a *PGK-Neo* cassette (Mahlapuu et al., 2001). The *Foxf1* locus was targeted in two ES cell lines: RW4, derived from 129/SvJ, and E14, derived from 129/Ola. Germline transmission was obtained with clones derived from both cell lines and the targeted allele was maintained on mixed 129/Ola-C57Bl/6, 129/Ola-CD1, 129/Sv-CD1 and 129/Sv-C57Bl/6 backgrounds. $Shh^{+/-}$ mice (Chiang et al., 1996) were obtained from The Jackson Laboratory, Maine (Stock Shh<tm1>, #JR3318).

In situ hybridization, immunohistochemistry, histology and skeletal preparations

Pregnant CD1 mice were sacrificed at different stages of gestation. The embryonic lungs were dissected in phosphate-buffered saline containing 0.1% Tween-20. The unfixed tissue was photographed immediately. For in situ hybridization and immunohistochemistry embryonic lungs were fixed in 4% paraformaldehyde at 4°C.

In situ hybridization of whole-mount embryos and cryosections (8 μm) or paraffin sections (3 μm) was performed as previously described (Blixt et al., 2000) using the following probes. The Foxf1 probe consists of a 400 bp *Not*I/*Ksp*I cDNA fragment located immediately 3′ of the forkhead box. Plasmids used to generate probes for uteroglobin (*Utg*; also known as *Cc10* or *Ccsp*) and surfactant proteins A, B and C (*Sftpa*, *Sftpb, Sftpc*) were kindly provided by Dr B. Stripp; for patched (*Ptch*) by Dr M. P. Scott; for *Foxa2* (*HNF3β*) and *Bmp4* by Dr B. L. M. Hogan; and for sonic hedgehog (*Shh*) by Dr C. Betsholtz. The probe for vascular smooth muscle α-actin (*Actvs*; now known as Acta2 – Mouse Genome Informatics) was generated from IMAGE cDNA clone No. 1224519. Immunostaining was performed with antibodies to platelet/endothelial cell adhesion molecule (Pecam; Pharmingen, clone MEC 13.3). Antibody binding was detected with biotinylated secondary antibodies and HRP-streptavidine amplified by TSA TM Biotin System (NEN Life Science Products). Histological sections (3 μm, paraffin) were stained with Eosin and Hematoxylin.

Bone and cartilage was visualized by staining with Alizarin Red and Alcian Blue (Hogan et al., 1994).

Whole lung organ cultures

Lung buds were dissected from E11.5 embryos and explants were placed on Millipore MF filters (Millipore), on top of stainless steel grids, in BGJb medium (Life Technologies) supplemented with 0.2 mg/ml ascorbic acid, 50 U/ml penicillin/streptomycin and 0.1% BSA. About 3 ml of medium was added to each 30 mm dish to establish an air-fluid interface at the level of the explants. The cultures were maintained in 5% CO_2, 100% humidity.

Localized effects of fibroblast growth factors (FGFs) in lung explant cultures were tested by implanting heparin beads (Sigma) impregnated with human recombinant FGF10 (100 μg/ml, R & D) or FGF7 (100 μg/ml, R & D) into the mesenchyme of E11.5 lungs, as described (Lebeche et al., 1999). The effect of human recombinant transforming growth factor β1 (TGFβ1; 7.5 μg/ml, R & D), TGFβ2 (50 μg/ml, R & D), bone morphogenetic protein 4 (BMP4; 100 μg/ml, R & D) and epidermal growth factor (EGF; 100 μg/ml, Sigma) in lung cultures was tested by grafting Affi-gel blue beads (BioRad) soaked in recombinant protein. Explants were cultured for 24 hours and fixed for whole-mount in situ hybridization.

Preparation of Shh-expressing cells

COS-7 cells were transfected with either sense or antisense (control) *Shh* expression plasmids (kindly provided by Dr J. Ericson) using LipofectAMINE (Life Technologies). After 24 hours, transfected cells were trypsinized and plated in bacteriological grade Petri dishes to generate aggregates of cells. Cell aggregates were implanted into E11.5 lung explants in whole lung organ cultures. Explants were incubated for 24 hours and fixed for whole-mount in situ hybridization.

RESULTS

Survival of *Foxf1* heterozygotes depends on genetic background

A *Foxf1*-null mutant was created by homologous recombination in embryonic stem (ES) cells (Mahlapuu et al., 2001). Chimeric mice that passed the targeted allele through germline were generated with cell clones obtained from two different ES cell lines – RW4 and E14 – derived from different inbred strains of mice, 129/SvJ and 129/Ola. Offspring from matings between chimeric males and C57Bl/6 females had the expected allele frequencies, consistent with Mendelian inheritance of the *Foxf1*-null allele (48% heterozygotes, n=67; see also Table 1). This frequency remained stable (50%, n=117) when first generation heterozygous males were crossed with C57Bl/6 females. In contrast, when chimeras were mated with CD1 females the frequency of heterozygous offspring was only 14.6% (n=137), indicating that approximately 83% of heterozygotes died before or soon after birth. Crosses between

Table 1. Genotype frequencies in offspring from crosses between *Foxf1* heterozygous males and females with different genetic backgrounds

Strain	Generation	Age	+/+	+/–
C57Bl/6	1	Born	35 (52%)	32 (48%)
	2	Born	59 (50%)	58 (50%)
CD1	1	Born	118 (86%)	19 (14%)
	1	E18.5	48 (44%)	62 (56%)
	2	Born	98 (93%)	7 (7%)

first generation survivor heterozygous males and CD1 females resulted in an even higher heterozygote mortality, estimated to be 93% (6.7% heterozygous pups, *n*=105). When fetuses were genotyped the day before birth, at E18.5, heterozygote frequency was normal (44%, *n*=110), which, together with the heterozygous genotype of dead newborn pups, showed that the low heterozygote frequency is due to perinatal mortality and not early resorbtion. Knockout lines established from the RW4 and E14 cell lines gave similar heterozygote frequencies and passing the targeted allele several generations through C57Bl/6 before crossing with CD1 did not alter this. The elevated perinatal mortality of *Foxf1* heterozygotes thus appears to reflect a sensitivity to *Foxf1* gene dose in the CD1 strain.

Foxf1 heterozygotes suffer from respiratory failure and foregut malformations

Anatomical and histological analysis of E18.5 *Foxf1* heterozygous fetuses from CD1 mothers revealed multiple malformations in the foregut and respiratory tract. The lungs are small and pale with hemorrhagic lesions along the edges (Fig. 1A). Instead of the four separate lobes of a normal right lung (Fig. 1B), various degrees of fusion between lobes are seen and one of the lobes – the accessory lobe – is consistently missing (Fig. 1A). Lung differentiation appears retarded; in some fetuses, formation of alveoli has not begun at E18.5, the lung mesenchyme is compact and looks undifferentiated (Fig. 1C,E). In others the histology looks normal, despite the smaller size and lobation defects of the lungs. In situ hybridization of E18.5 lung sections with probes for genes expressed in proximal (*Utg*) and distal (*Sftpa*, *Sftpb*, *Sftpc*) lung epithelium gave similar results in wild-type and *Foxf1* heterozygotes, which indicates that proximo-distal epithelial differentiation proceeds normally in the mutant (Fig. 1G-J and data not shown). No major alterations in lung vascularization could be detected, as judged by the expression pattern of markers for endothelial cells (platelet endothelial cell adhesion molecule type 1; Pecam1; Fig. 1K,M) and vascular smooth muscle cells (*Actvs*; Fig. 1L,N). However, a lower level of *Actvs* expression suggests that vascular smooth muscle differentiation may be hampered; something that could explain the hemorragic lesions in mutant lungs. Based on these results, and the fact that a fraction of *Foxf1* heterozygotes survive birth and reach maturity, we conclude that the mutants suffer from lung hypoplasia combined with a general and variable delay in lung maturation. The abnormal lobation indicates defects in lung branching morphogenesis.

In normal mouse development, the primordial lung buds and tracheal groove form around E9.5 as an epithelial outpouching from the ventral foregut, surrounded by splanchnic mesenchyme. The tracheo-esophageal septum divides the tracheal lumen and the foregut at E10.5, and by E11.5 trachea and esophagus are completely separated. The esophagus of E18.5 *Foxf1*$^{+/-}$ mutants has a narrow lumen (Fig. 2A), frequently merges with the trachea and sometimes ends before

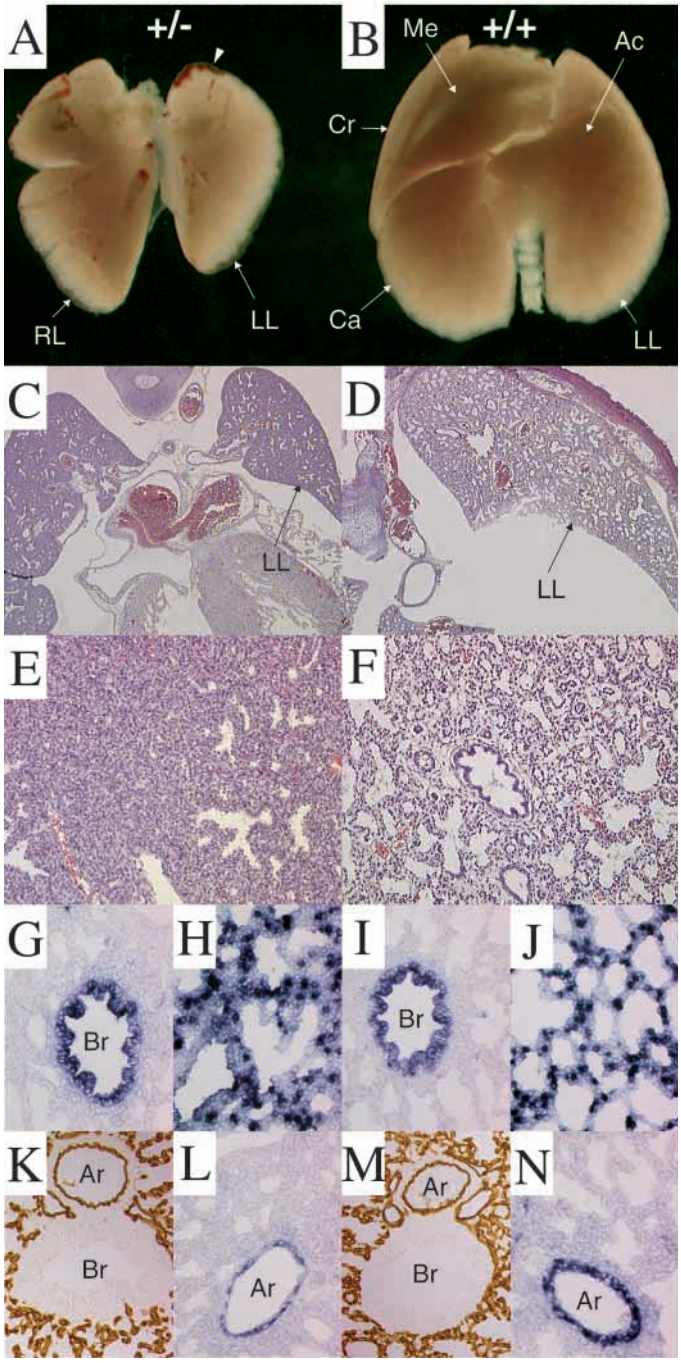

Fig. 1. Defects in lung lobation and maturation in *Foxf1*$^{+/-}$ embryos. (A,B) Ventral views of lungs from E18.5 wild-type and *Foxf1*$^{+/-}$ fetuses. The mutant lungs (A) are small, pale and have hemorrhagic lesions along the edges (arrowhead). The accessory lobe of the right lung is missing and the remaining lobes are partially fused. (C-F) Hematoxylin and Eosin staining of transversal sections from E18.5 *Foxf1*$^{+/-}$ (C,E) and wild-type (D,F) lungs. Low magnification view (C,D) shows the smaller size and denser appearance of the mutant lung. Higher magnification (E,F) reveals that the lax alveolar structure of the wild-type lung is replaced by compact mesenchyme in the *Foxf1* mutant. (G-N) Differentiation of epithelial and mesenchymal cells in E18.5 *Foxf1*$^{+/-}$ (G,H,K,L) and wild-type (I,J,M,N) lungs. In situ hybridization with probes for *Utg* (G,I), a marker for Clara cells of the proximal, bronchiolar epithelium, and *Sftpc* (H,J) expressed in the distal respiratory epithelium. Immunostaining of an endothelial cell marker (K,M; Pecam) and detection of vascular smooth muscle cells by in situ hybridization with a probe for *Actvs* (L,N). Ac, accessory lobe; Ar, arteriole; Br, bronchiole; Ca, caudal lobe; Cr, cranial lobe; LL, left lung; Me, medial lobe; RL, right lung.

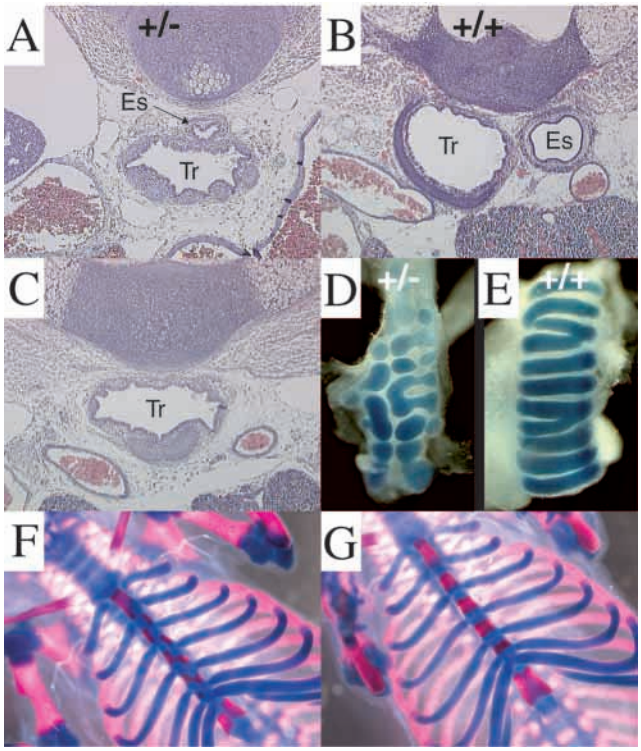

Fig. 2. Foregut, respiratory tract and skeletal malformations in *Foxf1*$^{+/-}$ embryos. (A-C) Hematoxylin and Eosin stained transversal sections showing trachea (Tr) and esophagus (Es) of E18.5 *Foxf1*$^{+/-}$ (A,C) and wild-type (B) fetuses. The mutants have variable degrees of narrowing of trachea and esophagus with esophageal atresia and a fistula-like fusion between esophagus and trachea. (D,E) Ventral view of Alcian Blue-stained tracheas from E18.5 *Foxf1*$^{+/-}$ (D) and wild-type (E) fetuses. The C-shaped cartilaginous rings, which are segmentally arranged along the trachea (E), are replaced by irregular, hypoplastic patches of cartilage in *Foxf1*$^{+/-}$ embryos (D; compare also B with A,C). (F,G) Skeletal malformation in *Foxf1*$^{+/-}$ mice shown by Alizarin Red and Alcian Blue staining of E18.5 fetuses. Attachment of the ribs to the sternum is asymmetrical in the mutant, and the ossification centra in the sternebrae (red staining parts of the sternum) are misaligned at the midline (F).

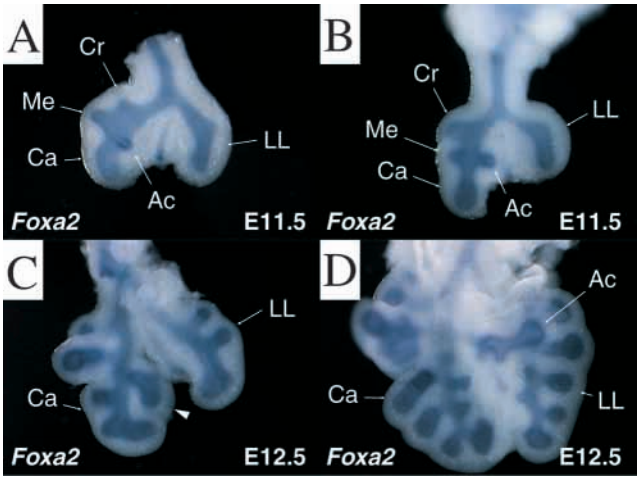

Fig. 3. (A-D) *Foxa2* whole-mount in situ hybridization of E11.5 (A,B) and E12.5 (C,D) *Foxf1*$^{+/-}$ (A,C) and wild-type (B,D) lungs. Primary epithelial branches of the right lung are formed normally at E11.5 in the mutant, although with a tendency of the buds to be wider proximally and less well defined (A). At E12.5, growth of the lungs and epithelial branching are retarded in mutant embryos (C) compared with wild type (D). The mesenchyme surrounding the accessory lobe epithelial bud of the mutant right lung remains fused with that of the caudal lobe (C; arrowhead), while a separate accessory lobe has already formed in wild-type embryos (D). Ac, accessory lobe; Ca, caudal lobe; Cr, cranial lobe; LL, left lung; Me, medial lobe.

reaching the pharynx (esophageal atresia; Fig. 2C). The tracheal cartilage of *Foxf1* heterozygotes is hypoplastic (Fig. 2A,C,D) and does not form the ventral rings typical of a normal trachea (Fig. 2B,E). The gastrointestinal tract posterior of the esophagus did not exhibit any anatomical or histological abnormalities.

Examination of the skeleton revealed that ribs are asymmetrically attached to the sternum in *Foxf1* mutant embryos (Fig. 2F). As a consequence, the bilateral ossification centra in the sternebrae are not aligned at the midline.

Based on the observed defects, we conclude that respiratory failure caused by lung immaturity and inability to feed, as a result of constriction or atresia of the esophagus, contributes to elevated perinatal mortality of *Foxf1* heterozygotes.

To investigate at what stage lung hypoplasia and lobation defects are first evident in *Foxf1* heterozygotes, we examined bud branching at the early stages of lung development. Lung epithelium was visualized by whole-mount in situ hybridization with a Foxa2 probe. At E11.5, the left and right lungs are separated by the primitive bronchi, and primary epithelial buds have developed that will give rise to the four lobes of the right lung (Fig. 3B). At this stage the branching pattern in *Foxf1* heterozygotes is similar to that in wild type, but with a tendency to form less well defined epithelial buds that are wider at the base (Fig. 3A). A day later, at E12.5, the respiratory tree has branched extensively in the wild type and the four lobes of the right lung are clearly distinguishable (Fig. 3D). Branching in the *Foxf1* mutant is considerably less advanced and separation of right lung lobes is incomplete (Fig. 3C). The mesenchyme surrounding the accessory lobe bud remains fused with the caudal lobe, which explains why a separate accessory lobe does not form (arrowhead in Fig. 3C).

Foxf1 is a target for Shh signaling

Foxf1 is expressed in the lung mesenchyme with the highest mRNA levels found adjacent to the epithelium (Mahlapuu et al., 1998). The expression pattern and the fact that *Foxf1* heterozygosity affects airway morphogenesis indicate that Foxf1 may take part in epithelio-mesenchymal crosstalk. Several observations suggest a functional connection between *Foxf1* and *Shh*. *Shh* is expressed throughout the epithelium (Bitgood and McMahon, 1995), but high level expression is restricted to the distal epithelium, in the growing buds (Fig. 4A; Bellusci et al., 1996; Urase et al., 1996). Target genes for Shh signaling, such as *Ptch*, show a complementary expression pattern, which is most prominent in the mesenchyme that surrounds the distal epithelium (Fig. 4B; Bellusci et al., 1997a). To investigate if *Foxf1* expression matches the sites of Shh secretion, we localized *Foxf1* mRNA in E11.5 and E12.5 lungs with whole-mount in situ hybridization. The results show that

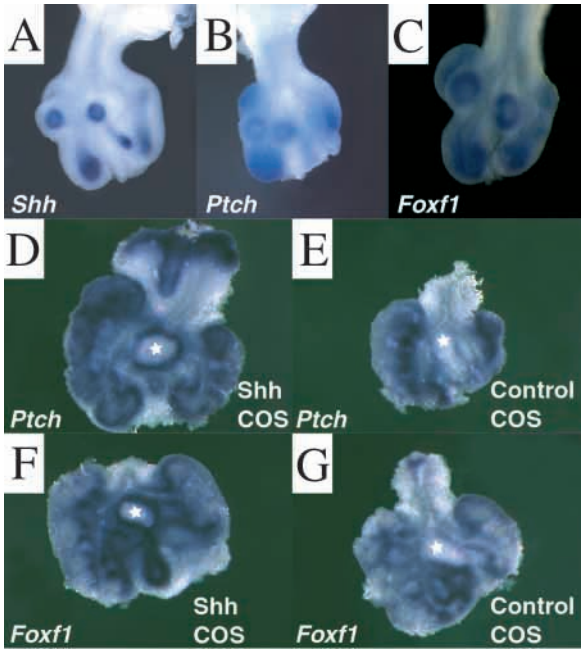

Fig. 4. *Foxf1* is a target for Sonic hedgehog signaling in lung. (A-C) Gene expression in E11.5 mouse lung examined by whole-mount in situ hybridization. *Shh* (A) is expressed throughout the lung epithelium, but the highest expression level is restricted to distal epithelium in the bulbous ends of the buds. *Ptch* (B), encoding the Shh receptor, and *Foxf1* (C) are both expressed in mesenchyme adjacent to lung epithelium. The expression patterns mirror the distribution of Shh, with low levels along the proximal tubular epithelium and higher levels distally. (D-G) Exogenous Shh activates *Foxf1*. COS-7 cells transfected to secrete Shh (D,F) or control COS-7 cells (E,G) were grafted into the mesenchyme (location of grafts indicated by white stars) of wild-type lung explants, which were then cultivated for 24 hours. The expression of *Ptch* (D,E) and *Foxf1* (F,G) were examined by whole-mount in situ hybridization. The mesenchyme immediately adjacent to the Shh-producing cells express elevated levels of both *Ptch* (D) and *Foxf1* (F), whereas no change is induced by control cells (E,G).

although expression of *Foxf1* is found in subepithelial mesenchyme throughout the airways, the highest level is confined to mesenchyme surrounding the distal epithelium of the buds (Fig. 4C). This pattern is similar to that of *Ptch* (Fig. 4B), which further supports the notion of a link between Shh signaling and *Foxf1* expression.

To determine if ectopic Shh secretion can activate *Foxf1* in lung mesenchyme, we used in vitro cultures of wild-type lung explants. COS-7 cells, transfected to secrete Shh, were implanted into the mesenchyme and the effects on expression of *Foxf1* was monitored by in situ hybridization. The expression of *Ptch* was also determined as an example of a mesenchymal target gene known to be activated by Shh. After 24 hours incubation, a zone of enhanced *Ptch* (Fig. 4D) and *Foxf1* (Fig. 4F) expression was seen surrounding the Shh-secreting cells, whereas no change in expression of either gene could be detected when control COS-7 cells were used (Fig. 4E,G). This result shows that transcriptional activation of *Foxf1* is a response of the lung mesenchyme to signaling by extracellular Shh.

If *Foxf1* transcription in lung mesenchyme is activated by Shh signaling, absence of Shh secretion from the endoderm should lead to downregulation of *Foxf1*. To test this, we investigated *Foxf1* expression in *Shh*$^{-/-}$ embryos. This mutant suffers from holoprosencephaly, cyclopia and defects in hair follicle, floorplate and limb development (Fig. 5G; Chiang et al., 1996; Litingtung et al., 1998; Pepicelli et al., 1998; St-Jacques et al., 1998). Lung growth and branching are retarded and mesenchymal expression of the Shh responsive genes *Ptch*, *Gli1*, *Gli3* and *Wnt2* is reduced (Litingtung et al., 1998; Pepicelli et al., 1998). The mesenchymal coating of the epithelium is thinner than in wild-type lungs (Fig. 5H; Litingtung et al., 1998; Pepicelli et al., 1998), consistent with Shh being a mesenchymal mitogen (Bellusci et al., 1997a). However, the mutant lung mesenchyme has a more widespread expression of *Fgf10* (Litingtung et al., 1998; Pepicelli et al., 1998), which is in agreement with other reports showing that Shh is a negative regulator of this gene (Bellusci et al., 1997b; Lebeche et al., 1999). Whole-mount in situ hybridization showed that in E10.5 and E12.5 *Shh*$^{-/-}$ embryos, *Foxf1* mRNA is absent from several of its normal sites of expression, including sclerotomes and mesenchyme of trachea, esophagus, oral cavity and lungs (Fig. 5). The midgut and hindgut, however, retain *Foxf1* expression pattern in *Shh* mutants (Fig. 5F,G). The lack of *Foxf1* expression in the lung mesenchyme and the splanchnic mesenchyme surrounding the foregut of E12.5 *Shh*$^{-/-}$ embryos, confirms that Shh signaling is required for activation of *Foxf1* in these tissues.

Foxf1 expression is downregulated by BMP4

A number of paracrine factors have been described to participate in the epithelio-mesenchymal crosstalk that controls morphogenesis and gene expression during early lung development (see Hogan, 1999; Hogan and Yingling, 1998). In order to identify other potential regulators of *Foxf1*, we investigated the effect of candidate growth factors on the *Foxf1* expression pattern in in vitro cultures of lung explants.

BMP4 is secreted by the distal epithelium of lung buds and inhibits epithelial branching and proliferation (Bellusci et al., 1996; Weaver et al., 1999). The distribution of *Foxf1* mRNA, which is lower adjacent to the *Bmp4*-expressing epithelium at the distal face of the bud than in a zone just behind the tip (compare Fig. 6B,D,H with Fig. 6F; see also Fig. 7B), suggests BMP4 as a potential negative regulator of *Foxf1*. To investigate the effect of BMP4 on *Foxf1* expression, we implanted BMP4-saturated beads in the mesenchyme of lung explants. As shown in Fig. 6A, exogenous BMP4 from a bead decreases *Foxf1* expression in the surrounding mesenchyme. Epithelial BMP4 is thus likely to act as a negative regulator of mesenchymal *Foxf1* expression. No change in *Foxf1* mRNA level or distribution was induced by TGFβ1 or TGFβ2, two additional members of the TGFβ superfamily that have been implicated in lung morphogenesis (Lebeche et al., 1999; Zhao et al., 1996), or by EGF, which is also essential for normal lung development (Miettinen et al., 1997; data not shown).

FGF10 and FGF7 are secreted by mesenchymal cells and signal through the FGFR2-IIIb receptor in the epithelium (Arman et al., 1999; De Moerlooze et al., 2000; Igarashi et al., 1998). As mesenchymal factors, FGFs are less likely to regulate *Foxf1* directly, but may do so indirectly through effects on epithelial gene expression. When added exogenously, in implanted beads, both FGF10 and FGF7 stimulate epithelial

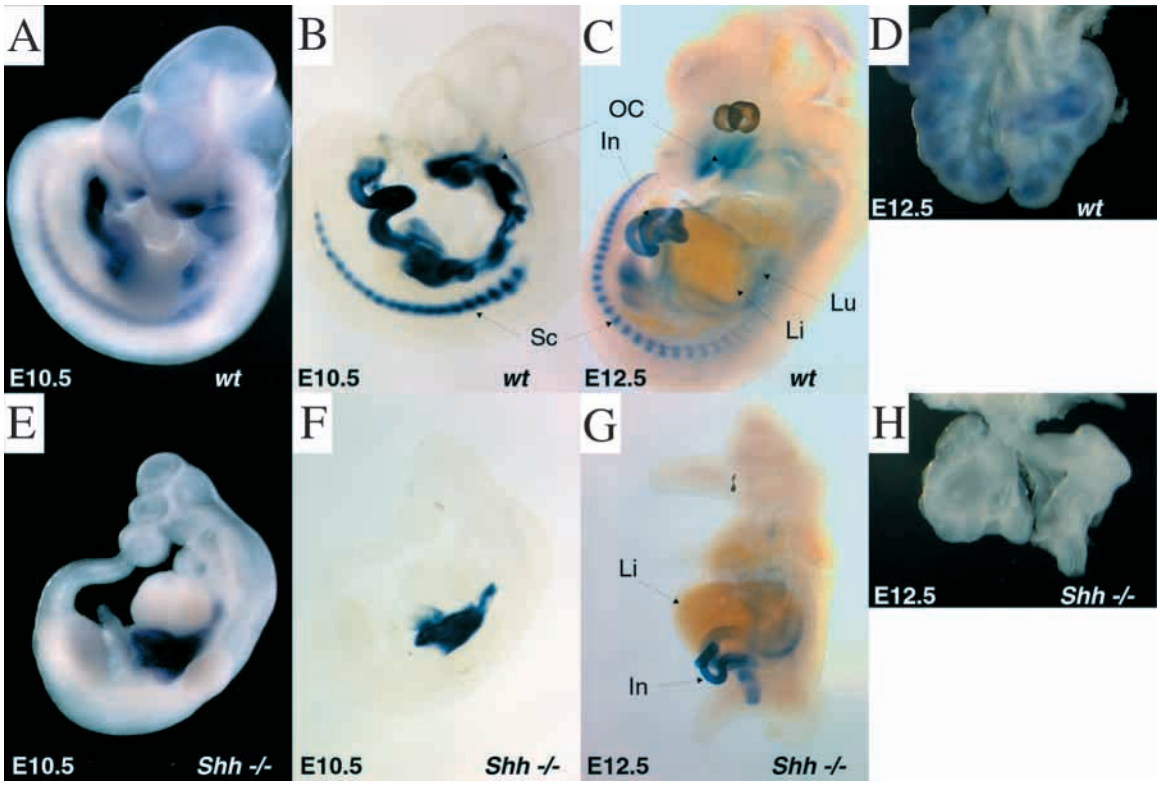

Fig. 5. Foregut and sclerotome expression of *Foxf1* depends on Shh. *Foxf1* whole-mount in situ hybridization of wild-type (A-D) and *Shh*$^{-/-}$ (E-H) E10.5 (A,B,E,F) or E12.5 (C,G) embryos and E12.5 lungs (D,H). In *Shh* mutants, *Foxf1* expression is missing in the anterior part of the gut, the oral cavity, in sclerotomes and lungs. *Foxf1* mRNA persists only in the posterior part of the gut, where *Ihh* is expressed. Embryos in A,E are in aqueous solution, to visualize the general morphology. Embryos in B,C,F,G are clarified in benzylalcohol:benzylacetate to show staining of internal structures. In, intestine; Li, liver; Lu, lung; OC, oral cavity; Sc, sclerotome.

proliferation and bud dilation, whereas the expression of *Foxf1* in subepithelial mesenchyme next to the bead decreases (Fig. 6C,G). FGF7 downregulates *Foxf1* in a wide area around the bead, adjacent to both proximal and distal epithelium (Fig. 6G). FGF7 also reduces expression of *Shh* in the epithelium (Fig. 6K; Lebeche et al., 1999) and *Ptch* in the mesenchyme (Fig. 6I). In the area influenced by exogenous FGF10, *Foxf1* is downregulated in the regions where it is normally expressed at high levels – next to distal epithelium – but the basal expression along the proximal, tubular epithelium is not affected (Fig. 6C). Distal epithelium also responds to exogenous FGF10 by activating *Bmp4* (Fig. 6E; Lebeche et al., 1999; Weaver et al., 2000).

DISCUSSION

Foxf1$^{-/-}$ embryos are deformed already at E8.5, never turn and die around E9.5, before organogenesis begins in the foregut (Mahlapuu et al., 2001). They cannot therefore be used to investigate the role of *Foxf1* in lung and gut morphogenesis. However, the heterozygous phenotype described here gives some insight into the normal function of *Foxf1* in this process. The fact that two independent targeted lines of mice, derived from ES cells of different genetic origin, produced the same phenotype and that the heterozygote frequency did not normalize during breeding, show that the observed defects are caused by the knockout. *Foxf1* haploinsufficiency depends on genetic background, which suggests that either the expression level or the threshold concentration of Foxf1 required for normal development varies between the tested strains. Although the nature of this variability is not known, the observed defects demonstrate the importance of *Foxf1* for normal foregut and lung development and also suggest links to upstream regulators.

The malformations seen in *Foxf1* heterozygotes bear a striking resemblance to those described for mutants in the Shh signaling pathway. Mice homozygous for null mutations in *Shh* have foregut defects with esophageal atresia or tracheo-esophageal fistula; lung growth is retarded and branching morphogenesis is impaired, but proximo-distal differentiation of the airway epithelium is unaffected (Litingtung et al., 1998; Pepicelli et al., 1998). Gli transcription factors are expressed in the lung mesenchyme and are nuclear targets for hedgehog signaling transduced from the patched/smoothened receptor (Dominguez et al., 1996; Goodrich et al., 1996; Tabin and McMahon, 1997). Mutations in genes for Gli proteins give rise to various lung and foregut defects. The *Gli2* knockout mice have narrowing of esophagus and trachea, tracheal cartilage dysplasia, small lungs with right lung lobe fusion and lack of accessory lobe (Motoyama et al., 1998). Heterozygosity for *Gli3* in a *Gli2*$^{-/-}$ background adds esophageal atresia with tracheo-esophageal fistula to the malformations and aggravates the lung hypoplasia (Motoyama et al., 1998). The similarities

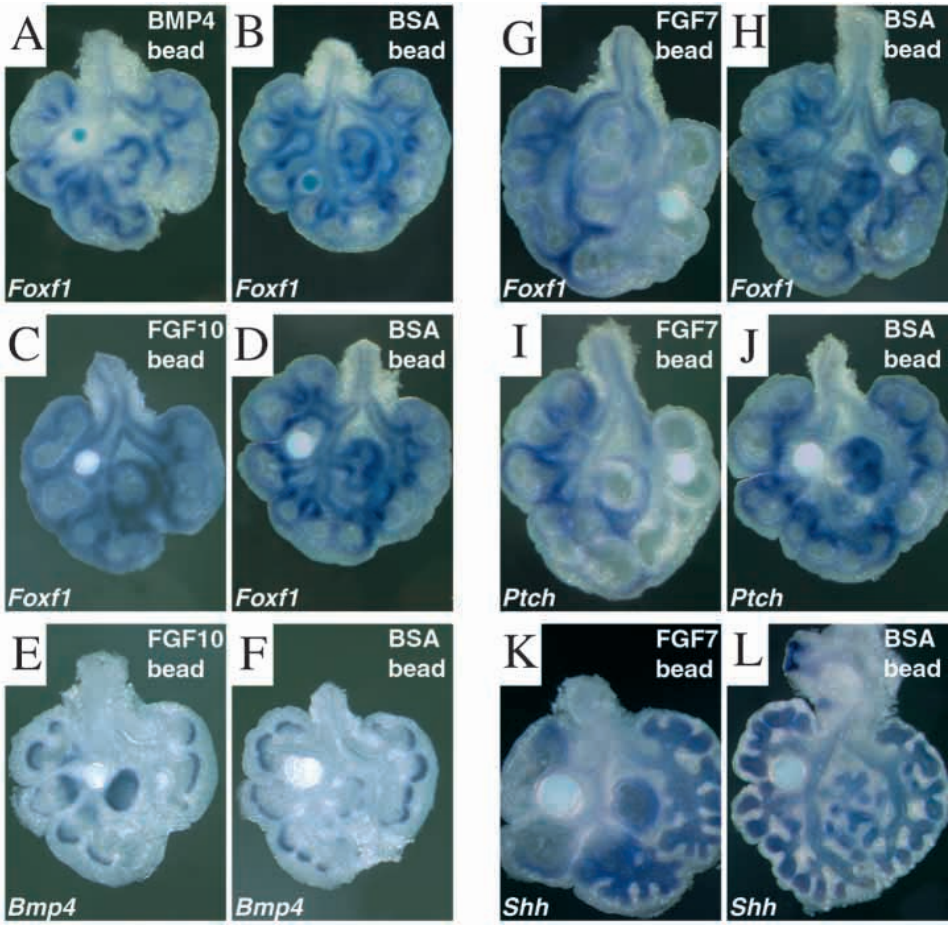

Fig. 6. *Foxf1* expression is downregulated by BMP4 and indirectly by FGF7 and FGF10. Beads soaked in BMP4 (A), FGF10 (C,E) or FGF7 (G,I,K) were implanted in the mesenchyme of wild-type lung explants, which were then cultivated for 24 hours. BSA-soaked beads served as a controls (B,D,F,H,J,L). Expression of *Foxf1* (A-D,G,H), *Bmp4* (E,F), *Ptch* (I,J) and *Shh* (K,L) was analyzed by whole-mount in situ hybridization. BMP4 reduces *Foxf1* expression in mesenchyme adjacent to the bead (A). FGF10 attracts distal epithelium and stimulates its proliferation, which is seen as dilation of the bulbous part of buds close to the bead (C). The patches of elevated *Foxf1* expression next to distal epithelium (D) are lost in the area influenced by exogenous FGF10 (C), whereas no effect is seen on the low level expression in mesenchyme along the proximal, tubular epithelium (C). A likely explanation for this inhibition is that it is mediated by BMP4, as *Bmp4* is activated by FGF10 in distal, but not in proximal epithelium (E). FGF7 induces an even more pronounced epithelial proliferation and bud expansion (G,I,K). *Foxf1* is generally downregulated in the area influenced by FGF7 (G), which may be mediated by a decreased Shh signaling, as epithelial *Shh* expression is reduced by FGF7 (K). This interpretation is supported by the similarity in the effect of FGF7 on *Foxf1* and another Shh-responsive gene, *Ptch* (I).

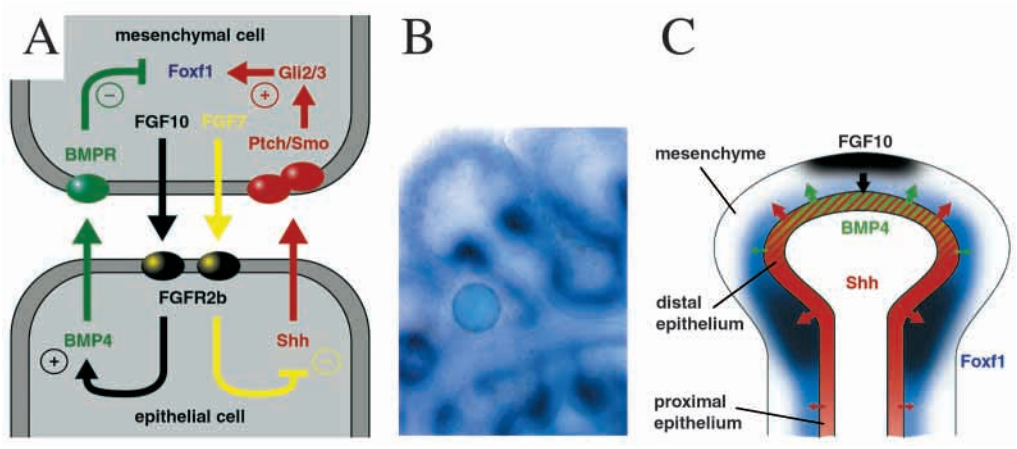

Fig. 7. Summary of paracrine interactions shaping the *Foxf1* expression pattern in developing lung. (A) Activation of *Foxf1* by Shh is based on both ectopic expression and loss-of-function experiments presented in this work. The inclusion of *Gli2/3* in this pathway is inferred from their role in transducing the hedgehog signal and the similarity between *Gli2/3* knockout phenotypes and the *Foxf1* heterozygote phenotype. Inhibition by BMP4 refers to the effect of BMP4 beads on *Foxf1* expression presented here. The role of FGF10 and FGF7 in regulation of *Bmp4* and *Shh*, respectively, has been published by others (Lebeche et al., 1999) and has also been confirmed by us; the net effect of FGFs on *Foxf1* expression was analyzed in this work. (B) High magnification view of lung explant hybridized with a Foxf1 probe. *Foxf1* expression in subepithelial mesenchyme peaks at the transition between the proximal, tubular epithelium the distal, bulbous part of the bud. The circular object is a bead implanted in the mesenchyme as a negative control and has no relevance for the expression pattern discussed here. (C) Model of paracrine signaling in a lung bud that provides a possible explanation for the observed distribution of *Foxf1* mRNA. Proximal tubular epithelium secretes a low level of Shh (pink), which gives rise to a low level of *Foxf1* expression (light blue) in the subepithelial mesenchyme. Shh secretion is higher in the distal epithelium (red), which activates high level expression of *Foxf1* (dark blue). *Fgf10* is expressed in mesenchyme at the distal tip of the bud (black). In response to FGF10 signaling, *Bmp4* is activated in the most distal epithelium (green). Secretion of BMP4 inhibits *Foxf1* expression, which therefore drops again towards the tip of the bud (light blue).

of the mutant phenotypes suggest that *Shh*, *Gli* and *Foxf1* are parts of the same signaling pathway. The mesenchymal expression of *Foxf1*, its activation by ectopic Shh secretion and loss of expression in *Shh*$^{-/-}$ lung bud mesenchyme place *Foxf1* downstream of *Shh*. Ci, the *Drosophila* homolog of mammalian *Gli* genes, encodes a protein whose activity as transcription factor is regulated directly by hedgehog signaling (Dominguez et al., 1996). It is therefore likely that *Foxf1* is downstream of *Gli* in mammals and perhaps directly transcriptionally activated by Gli proteins (Fig. 7A).

Shh is expressed in axial structures, floorplate and notochord (Echelard et al., 1993), where it is involved in somite patterning and formation of sclerotomes from cells of the ventromedial part of the somites (Fan et al., 1995; Fan and Tessier-Lavigne, 1994; Johnson et al., 1994). In *Shh*$^{-/-}$ embryos that develop to term, most sclerotomal derivatives, including the entire vertebral column, are absent (Chiang et al., 1996). However, sclerotomal differentiation in *Shh* mutant embryos is initiated normally, as judged by expression of the sclerotomal marker *Pax1* (Chiang et al., 1996). Based on this, Shh is postulated to be essential for the maintenance, but not the initiation, of sclerotome differentiation (Chiang et al., 1996; Marcelle et al., 1999). *Foxf1* is not expressed in somites, but is turned on in sclerotomal cells as these separate from the dermomyotome (Mahlapuu et al., 2001). As development of the axial skeleton proceeds, *Foxf1* is turned off in the condensed, chondrogenic mesenchyme of the future vertebra and remains expressed in the gradually narrowing intervertebral discs (Fig. 5B,C; Aitola et al., 2000; Mahlapuu et al., 2001; Mahlapuu et al., 1998). In *Shh*$^{-/-}$ embryos, no sclerotomal expression of *Foxf1* is observed, which is consistent with our conclusion that *Foxf1* is a target for Shh signaling. This also shows that although *Pax1* is induced normally in the *Shh* mutant and apparently can be activated by a Shh-independent pathway, other sclerotomal markers – such as *Foxf1* – are not. Thus, Shh is necessary for specific aspects of sclerotome induction and not just for maintenance.

The absence of *Foxf1* expression in sclerotomes and in mesenchyme surrounding the foregut epithelium and lung buds of *Shh*$^{-/-}$ embryos, indicates that transcriptional activation of *Foxf1* is a response to Shh signaling in these tissues. In contrast, the midgut and hindgut expression of *Foxf1* is normal in the *Shh* mutant. The expression range of *Foxf1* in gut mesenchyme of *Shh*$^{-/-}$ embryos exactly matches the expression of another member of the hedgehog family, *Ihh*. Ihh signals via the same receptor as Shh and is expressed in gut epithelium from the hindstomach to the rectum (Bitgood and McMahon, 1995). It is thus possible that activation by hedgehog signaling is a general requirement for *Foxf1* expression. Indeed, throughout embryonic development, expression of *Foxf1* correlates with sites of hedgehog secretion. In addition to the gut, lungs and sclerotomes, *Foxf1* is also expressed in the subepithelial mesenchyme of the oral cavity, the tongue and dental follicles (Aitola et al., 2000; Mahlapuu et al., 2001; Mahlapuu et al., 1998), all of which are proximal to sites of epithelial Shh production (Bitgood and McMahon, 1995). At the early somite stage, *Foxf1* is expressed in extra-embryonic mesoderm, including the yolk sac blood islands (Mahlapuu et al., 2001; Peterson et al., 1997); an expression pattern that it shares with *Ptch* (Maye et al., 2000) and which matches the secretion of *Ihh* from the yolk sac endoderm (Farrington et al., 1997; Maye et al., 2000). In the patterning of primitive mesoderm, *Foxf1* expression characterizes the lateral plate mesoderm, which is adjacent to regions of visceral endoderm that produce *Shh* and *Ihh* (Echelard et al., 1993).

Asymmetry of rib attachment and in ossification of the sternum is a common malformation in *Foxf1* heterozygotes. This represents an exaggerated version of the ‘crankshaft sternum’ (Theiler, 1989), which can also be caused by inactivation of engrailed 1 (Wurst et al., 1994) and by experimental amniotic sac puncture (Chang et al., 1996). The connection between *Foxf1* gene dose and sternal morphogenesis is not clear, as *Foxf1* is expressed neither in the sternal, nor the costal, primordia. As discussed above, *Foxf1* is expressed in sclerotomal mesenchyme and is turned off during chondroblast differentiation (Aitola et al., 2000; Mahlapuu et al., 2001; Mahlapuu et al., 1998). It is possible that a reduced expression level of *Foxf1* could induce a subtle vertebral asymmetry that causes the left and right costal processes to grow at slightly different angles. Another possibility is that the composition of the amniotic fluid is altered in response to a lowered *Foxf1* expression. *Foxf1* is expressed in amnion (Peterson et al., 1997) and is essential for its development and function; in homozygous *Foxf1* knockout embryos the mesodermal component of the amnion has severe defects in differentiation and cell adhesion (Mahlapuu et al., 2001). Finally, the skeletal defects may be secondary to the altered chest morphology that is a consequence of a considerable reduction in lung volume.

Bmp4 is expressed in the distal face of the epithelial buds of the developing lung and is induced by FGF10 signaling from the adjacent mesenchyme (Lebeche et al., 1999; Weaver et al., 2000). The stimulation of epithelial cell proliferation, caused by FGF10, is counteracted by BMP4 (Weaver et al., 2000). Locally applied BMP4 has an inhibitory effect on mesenchymal *Foxf1* expression in lung explants. Lowering the *Foxf1* expression by reducing its gene dose, as in *Foxf1* heterozygotes, may therefore have similar effects as an increase in *Bmp4* expression. In fact, epithelial overexpression of *Bmp4* in transgenic mice results in lung hypoplasia, inhibition of branching, and pulmonary immaturity at birth (Bellusci et al., 1996).

FGF10 is produced by groups of mesenchymal cells located distally of the epithelial buds (Bellusci et al., 1997b) and activates *Bmp4* expression in the adjacent epithelium. It functions as a mitogen and a chemoattractant for epithelial cells and induce bud dilation when provided exogenously (Bellusci et al., 1997b; Park et al., 1998). *Fgf10* is essential for lung bud formation and branching; *Fgf10*$^{-/-}$ embryos develop trachea, but no lungs (Min et al., 1998; Sekine et al., 1999). In response to implantation of a bead containing FGF10, mesenchymal cells adjacent to bud epithelium express less *Foxf1*. A likely mechanism behind the decrease in *Foxf1* expression in response to FGF10 is enhanced inhibition by BMP4, as *Bmp4* expression increases in bud epithelium next to the bead (Fig. 6A). This interpretation is supported by the observation that *Foxf1* expression is only downregulated in the sites of high expression, next to the bud epithelium. Along the proximal, tubular epithelium of the future bronchi, *Foxf1* expression is normal. This is exactly the pattern that would be expected if the effect was mediated by BMP4, as, unless the mesenchyme is removed experimentally, FGF10 activates

Bmp4 only in bud epithelium, not in proximal tubular epithelium (Lebeche et al., 1999; Weaver et al., 2000).

A second FGF family member, FGF7, is also produced by the lung mesenchyme. The effect on epithelium induced by FGF7 is distinct from that of FGF10, although both factors signal through the same receptor, FGFR2-IIIb (Arman et al., 1999; De Moerlooze et al., 2000; Igarashi et al., 1998). *Shh* expression is inhibited by FGF7, but not by FGF10 (Lebeche et al., 1999). Locally applied exogenous FGF7 decreases *Foxf1* expression. As Shh activates *Foxf1*, decreased activation by Shh signaling is a plausible mechanism behind the reduced expression of *Foxf1* seen in response to exogenous FGF7. A reduction in *Ptch* expression similar to that observed for *Foxf1* in the area influenced by FGF7 is consistent with this interpretation (Fig. 6I; Lebeche et al., 1999). The paracrine interactions thought to influence *Foxf1* expression in the lung are summarized in Fig. 7A.

A low level of *Foxf1* mRNA is found in a zone of mesenchyme that lines the proximal, tubular epithelium of the developing lung (Fig. 7B); an expression pattern that matches the basal level of *Shh* expression in this part of the epithelial tree. In the buds, the expression level of *Shh* is significantly higher, which will upregulate *Foxf1* in the surrounding mesenchyme. At the same time, BMP4 secreted from the distal epithelium of the bud will inhibit *Foxf1* expression. However, whereas *Bmp4* expression is confined to the most distal part of the bud, *Shh* expression is elevated in the entire bulbous part and thus extends further proximally. These interactions may explain the observed distribution of *Foxf1* mRNA, which peaks at the transition between the distal, bulbous and the proximal, tubular epithelium and then falls back to a lower level along the outer, distal face of the bud (Fig. 7B,C).

An important question that remains to be answered is what target genes are regulated by Foxf1 and the role that it plays in formation of the lung. The expression pattern suggests that Foxf1 could be involved in reshaping the growing bud into a narrower, tubular shape (Fig. 7B). Heterozygous lungs exhibit a general growth retardation, which suggests that *Foxf1* promotes proliferation. Shh is a mesenchymal mitogen (Bellusci et al., 1997a) and this function may be mediated by *Foxf1*. The notion that *Foxf1* can be involved in growth control is supported by the observation that proliferation of primitive streak mesoderm is reduced in *Foxf1*$^{-/-}$ embryos (Mahlapuu et al., 2001).

Their phenotypical similarity with *Foxf1* heterozygotes suggests that *Shh*, *Gli2* and *Gli3* mutants owe many of their malformations to a reduction in *Foxf1* expression, thus implicating *Foxf1* as a key target of hedgehog signaling in lung and foregut morphogenesis. Although the phenotype depends on genetic background, it shows that *Foxf1* gene dose can be crucial for developmental processes. In humans, foregut malformations including esophageal atresia, tracheo-esophageal fistula and lung anomalies occur in 1 in 2000-5000 live births (Skandalakis and Gray, 1994). The human *FOXF1* gene, located at 16q24 (Larsson et al., 1995), should be considered a candidate locus in familial cases of these malformations.

We would like to thank Drs B. L. M. Hogan, B. Stripp, M. P. Scott, J. Ericson and C. Betsholtz for plasmid clones and Amel Linde for technical advice on organ culture. This work was supported by a grant to P. C. from the Swedish Cancer Foundation.

REFERENCES

Aitola, M., Carlsson, P., Mahlapuu, M., Enerbäck, S. and Pelto-Huikko, M. (2000). Forkhead transcription factor FoxF2 is expressed in mesodermal tissues involved in epithelio-mesenchymal interactions. *Dev. Dyn.* **18**, 136-149.

Arman, E., Haffner-Krausz, R., Gorivodsky, M. and Lonai, P. (1999). Fgfr2 is required for limb outgrowth and lung-branching morphogenesis. *Proc. Natl. Acad. Sci. USA* **96**, 11895-11899.

Aza-Blanc, P. and Kornberg, T. B. (1999). Ci: a complex transducer of the hedgehog signal. *Trends Genet.* **15**, 458-462.

Bellusci, S., Henderson, R., Winnier, G., Oikawa, T. and Hogan, B. L. (1996). Evidence from normal expression and targeted misexpression that bone morphogenetic protein (Bmp-4) plays a role in mouse embryonic lung morphogenesis. *Development* **122**, 1693-1702.

Bellusci, S., Furuta, Y., Rush, M. G., Henderson, R., Winnier, G. and Hogan, B. L. (1997a). Involvement of Sonic hedgehog (Shh) in mouse embryonic lung growth and morphogenesis. *Development* **124**, 53-63.

Bellusci, S., Grindley, J., Emoto, H., Itoh, N. and Hogan, B. L. (1997b). Fibroblast growth factor 10 (FGF10) and branching morphogenesis in the embryonic mouse lung. *Development* **124**, 4867-4878.

Bitgood, M. J. and McMahon, A. P. (1995). Hedgehog and Bmp genes are coexpressed at many diverse sites of cell- cell interaction in the mouse embryo. *Dev. Biol.* **172**, 126-138.

Blixt, Å., Mahlapuu, M., Aitola, M., Pelto-Huikko, M., Enerbäck, S. and Carlsson, P. (2000). A forkhead gene, *FoxE3*, is essential for lens epithelial proliferation and closure of the lens vesicle. *Genes Dev.* **14**, 245-254.

Chang, H. H., Schwartz, Z. and Kaufman, M. H. (1996). Limb and other postcranial skeletal defects induced by amniotic sac puncture in the mouse. *J. Anat.* **189**, 37-49.

Chiang, C., Litingtung, Y., Lee, E., Young, K. E., Corden, J. L., Westphal, H. and Beachy, P. A. (1996). Cyclopia and defective axial patterning in mice lacking Sonic hedgehog gene function. *Nature* **383**, 407-413.

Clevidence, D. E., Overdier, D. G., Peterson, R. S., Porcella, A., Ye, H., Paulson, K. E. and Costa, R. H. (1994). Members of the HNF-3/forkhead family of transcription factors exhibit distinct cellular expression patterns in lung and regulate the surfactant protein B promoter. *Dev. Biol.* **166**, 195-209.

De Moerlooze, L., Spencer-Dene, B., Revest, J., Hajihosseini, M., Rosewell, I. and Dickson, C. (2000). An important role for the IIIb isoform of fibroblast growth factor receptor 2 (FGFR2) in mesenchymal-epithelial signalling during mouse organogenesis. *Development* **127**, 483-492.

Dominguez, M., Brunner, M., Hafen, E. and Basler, K. (1996). Sending and receiving the hedgehog signal: control by the Drosophila Gli protein Cubitus interruptus. *Science* **272**, 1621-1625.

Echelard, Y., Epstein, D. J., St-Jacques, B., Shen, L., Mohler, J., McMahon, J. A. and McMahon, A. P. (1993). Sonic hedgehog, a member of a family of putative signaling molecules, is implicated in the regulation of CNS polarity. *Cell* **75**, 1417-1430.

Fan, C. M., Porter, J. A., Chiang, C., Chang, D. T., Beachy, P. A. and Tessier-Lavigne, M. (1995). Long-range sclerotome induction by sonic hedgehog: direct role of the amino-terminal cleavage product and modulation by the cyclic AMP signaling pathway. *Cell* **81**, 457-465.

Fan, C. M. and Tessier-Lavigne, M. (1994). Patterning of mammalian somites by surface ectoderm and notochord: evidence for sclerotome induction by a hedgehog homolog. *Cell* **79**, 1175-1186.

Farrington, S. M., Belaoussoff, M. and Baron, M. H. (1997). Winged-helix, Hedgehog and Bmp genes are differentially expressed in distinct cell layers of the murine yolk sac. *Mech. Dev.* **62**, 197-211.

Goodrich, L. V., Johnson, R. L., Milenkovic, L., McMahon, J. A. and Scott, M. P. (1996). Conservation of the hedgehog/patched signaling pathway from flies to mice: induction of a mouse patched gene by Hedgehog. *Genes Dev.* **10**, 301-312.

Hellqvist, M., Mahlapuu, M., Samuelsson, L., Enerbäck, S. and Carlsson, P. (1996). Differential activation of lung-specific genes by two forkhead proteins, FREAC-1 and FREAC-2. *J. Biol. Chem.* **271**, 4482-4490.

Hellqvist, M., Mahlapuu, M., Blixt, Å., Enerbäck, S. and Carlsson, P. (1998). The human forkhead protein FREAC-2 contains two functionally redundant activation doamins and interacts with TBP and TFIIB. *J. Biol. Chem.* **273**, 23335-23343.

Hogan, B., Beddington, R., Costantini, F. and Lacy, E. (1994). *Manipulating the Mouse Embryo*: *A Laboratory Manual*. New York: Cold Spring Harbor Laboratory Press.

Hogan, B. L. (1999). Morphogenesis. *Cell* **96**, 225-233.

Hogan, B. L. and Yingling, J. M. (1998). Epithelial/mesenchymal interactions and branching morphogenesis of the lung. *Curr. Opin. Genet. Dev.* **8**, 481-486.

Igarashi, M., Finch, P. W. and Aaronson, S. A. (1998). Characterization of recombinant human fibroblast growth factor (FGF)-10 reveals functional similarities with keratinocyte growth factor (FGF-7). *J. Biol. Chem.* **273**, 13230-13235.

Johnson, R. L., Laufer, E., Riddle, R. D. and Tabin, C. (1994). Ectopic expression of Sonic hedgehog alters dorsal-ventral patterning of somites. *Cell* **79**, 1165-1173.

Larsson, C., Hellqvist, M., Pierrou, S., White, I., Enerbäck, S. and Carlsson, P. (1995). Chromosomal localization of six human forkhead genes, freac-1, -3, -4, -5, -6 and -8. *Genomics* **30**, 464-469.

Lebeche, D., Malpel, S. and Cardoso, W. V. (1999). Fibroblast growth factor interactions in the developing lung. *Mech. Dev.* **86**, 125-136.

Litingtung, Y., Lei, L., Westphal, H. and Chiang, C. (1998). Sonic hedgehog is essential to foregut development. *Nat. Genet.* **20**, 58-61.

Mahlapuu, M., Pelto-Huikko, M., Aitola, M., Enerbäck, S. and Carlsson, P. (1998). FREAC-1 contains a cell type-specific transcriptional activation domain and is expressed in epithelial-mesenchymal interfaces. *Dev. Biol.* **202**, 183-195.

Mahlapuu, M., Ormestad, M., Enerbäck, S. and Carlsson, P. (2001). The forkhead transcription factor *Foxf1* is required for differentiation of extraembryonic and lateral plate mesoderm. *Development* **128**, 155-166.

Marcelle, C., Ahlgren, S. and Bronner-Fraser, M. (1999). In vivo regulation of somite differentiation and proliferation by Sonic Hedgehog. *Dev. Biol.* **214**, 277-287.

Maye, P., Becker, S., Kasameyer, E., Byrd, N. and Grabel, L. (2000). Indian hedgehog signaling in extraembryonic endoderm and ectoderm differentiation in ES embryoid bodies. *Mech. Dev.* **94**, 117-132.

McMahon, A. P. (2000). More surprises in the Hedgehog signaling pathway. *Cell* **100**, 185-188.

Miettinen, P. J., Warburton, D., Bu, D., Zhao, J. S., Berger, J. E., Minoo, P., Koivisto, T., Allen, L., Dobbs, L., Werb, Z. et al. (1997). Impaired lung branching morphogenesis in the absence of functional EGF receptor. *Dev. Biol.* **186**, 224-236.

Min, H., Danilenko, D. M., Scully, S. A., Bolon, B., Ring, B. D., Tarpley, J. E., DeRose, M. and Simonet, W. S. (1998). Fgf-10 is required for both limb and lung development and exhibits striking functional similarity to Drosophila branchless. *Genes Dev.* **12**, 3156-3161.

Motoyama, J., Liu, J., Mo, R., Ding, Q., Post, M. and Hui, C. C. (1998). Essential function of Gli2 and Gli3 in the formation of lung, trachea and oesophagus. *Nat. Genet.* **20**, 54-57.

Park, W. Y., Miranda, B., Lebeche, D., Hashimoto, G. and Cardoso, W. V. (1998). FGF-10 is a chemotactic factor for distal epithelial buds during lung development. *Dev. Biol.* **201**, 125-134.

Park, H. L., Bai, C., Platt, K. A., Matise, M. P., Beeghly, A., Hui, C. C., Nakashima, M. and Joyner, A. L. (2000). Mouse Gli1 mutants are viable but have defects in SHH signaling in combination with a Gli2 mutation. *Development* **127**, 1593-1605.

Pepicelli, C. V., Lewis, P. M. and McMahon, A. P. (1998). Sonic hedgehog regulates branching morphogenesis in the mammalian lung. *Curr. Biol.* **8**, 1083-1086.

Peterson, R. S., Lim, L., Ye, H., Zhou, H., Overdier, D. G. and Costa, R. H. (1997). The winged helix transcriptional activator HFH-8 is expressed in the mesoderm of the primitive streak stage of mouse embryos and its cellular derivatives. *Mech. Dev.* **69**, 53-69.

Pierrou, S., Hellqvist, M., Samuelsson, L., Enerbäck, S. and Carlsson, P. (1994). Cloning and characterization of seven human forkhead proteins: binding site specificity and DNA bending. *EMBO J.* **13**, 5002-5012.

Sekine, K., Ohuchi, H., Fujiwara, M., Yamasaki, M., Yoshizawa, T., Sato, T., Yagishita, N., Matsui, D., Koga, Y., Itoh, N. et al. (1999). Fgf10 is essential for limb and lung formation. *Nat. Genet.* **21**, 138-141.

Skandalakis, J. E. and Gray, S. W. (1994). *Embryology for Surgeons.* Baltimore, MD: Williams & Wilkins.

St-Jacques, B., Dassule, H. R., Karavanova, I., Botchkarev, V. A., Li, J., Danielian, P. S., McMahon, J. A., Lewis, P. M., Paus, R. and McMahon, A. P. (1998). Sonic hedgehog signaling is essential for hair development. *Curr. Biol.* **8**, 1058-1068.

Tabin, C. J. and McMahon, A. P. (1997). Recent advances in Hedgehog signaling. *Trends Cell Biol.* **7**, 442-446.

Theiler, K. (1989). *The House Mouse: Atlas of Embryonic Development*. New York: Springer-Verlag.

Urase, K., Mukasa, T., Igarashi, H., Ishii, Y., Yasugi, S., Momoi, M. Y. and Momoi, T. (1996). Spatial expression of Sonic hedgehog in the lung epithelium during branching morphogenesis. *Biochem. Biophys. Res. Commun.* **225**, 161-166.

Weaver, M., Dunn, N. R. and Hogan, B. L. (2000). Bmp4 and Fgf10 play opposing roles during lung bud morphogenesis. *Development* **127**, 2695-2704.

Weaver, M., Yingling, J. M., Dunn, N. R., Bellusci, S. and Hogan, B. L. (1999). Bmp signaling regulates proximal-distal differentiation of endoderm in mouse lung development. *Development* **126**, 4005-4015.

Wessells, N. K. (1970). Mammalian lung development: interactions in formation and morphogenesis of tracheal buds. *J. Exp. Zool.* **175**, 455-466.

Wurst, W., Auerbach, A. B. and Joyner, A. L. (1994). Multiple developmental defects in Engrailed-1 mutant mice: an early mid-hindbrain deletion and patterning defects in forelimbs and sternum. *Development* **120**, 2065-2075.

Zhao, J., Bu, D., Lee, M., Slavkin, H. C., Hall, F. L. and Warburton, D. (1996). Abrogation of transforming growth factor-beta type II receptor stimulates embryonic mouse lung branching morphogenesis in culture. *Dev. Biol.* **180**, 242-257.